

Observational constraints on viscous free- γ fluid in $f(Q)$ gravity

Simran Arora^{1,*}, Sai Swagat Mishra^{2,†} and P. K. Sahoo^{3,‡}

¹Center for Gravitational Physics and Quantum Information,

Yukawa Institute for Theoretical Physics, Kyoto University, 606-8502, Kyoto, Japan.

²Department of Mathematics, School of Computer Science and Artificial Intelligence,
SR University, Warangal 506371, Telangana, India

³Department of Mathematics, Birla Institute of Technology and Science, Pilani,
Hyderabad Campus, Jawahar Nagar, Kapra Mandal, Medchal District, Telangana 500078, India

We study the late-time cosmological dynamics of a spatially flat FLRW universe in the framework of $f(Q)$ gravity, where Q denotes the nonmetricity scalar. The matter sector is modeled as a bulk viscous fluid with a free equation-of-state parameter γ , allowing for a generalized description of cosmic matter beyond the standard dust approximation. We derive the background evolution equations and analyze the resulting expansion history. The model parameters are constrained using a combination of observational datasets, including cosmic chronometers (CC), baryon acoustic oscillations from DESI DR2, and Type Ia supernovae (GRBs and Union3). Using the best-fit parameters, we further employ the statefinder and $\text{Om}(z)$ diagnostics to distinguish the viscous $f(Q)$ scenario from the standard Λ CDM model. In addition, we examine the evolution of the deceleration parameter, which exhibits a transition from an early decelerated phase to the current accelerated expansion, and analyze the effective equation-of-state behavior. Our results show that bulk viscosity within $f(Q)$ gravity provides a viable and observationally consistent description of late-time cosmic acceleration.

Keywords: Modified gravity—observations—viscous free- γ —dark energy

I. INTRODUCTION

Observations over the past few decades have established a coherent picture of the late-time Universe as undergoing accelerated expansion. This conclusion is primarily supported by measurements from Type Ia supernovae (SNeIa) [1, 2], large-scale structure surveys [3, 4], baryon acoustic oscillations (BAO) [5–8] and cosmic microwave background [9].

Within the framework of general relativity (GR), the most standard explanation for this phenomenon is the presence of a cosmological constant, described by a constant and negative equation-of-state parameter. This interpretation underlies the standard Λ CDM model, which has achieved notable success in reproducing a wide range of late-time observational data. Despite this success, the cosmological constant is plagued by a serious theoretical difficulty: its observed value is many orders of magnitude smaller than that predicted by quantum field theory and the requirement of finely tuned initial conditions [10, 11]. These shortcomings provide strong motivation to explore alternatives to a strictly constant dark-energy component. In this context, modifications and extensions of GR offer a natural framework in which cosmic acceleration can emerge dynamically at late times, while remaining compatible with constraints from low-redshift observations.

Amongst studies aiming to provide an alternative explanation for the effects of dark energy, modified theories based on curvature ($f(R)$ gravity) and torsion ($f(T)$ gravity and its extensions) have received special attention in recent years [12–19]. In light of the geometrical nature of gravity, it is essential to investigate the various geometrical forms that gravity might assume. The nonmetricity is the other fundamental characteristic connected to the connection, in addition to curvature and torsion. It has been suggested to create conditions where the gravitational interaction is mediated by nonmetricity, whereas curvature and torsion are vanishing, among other strong candidates for modified gravity theories. This gives us symmetric teleparallel gravity, further extended to $f(Q)$ gravity

* dawrasimran27@gmail.com, arora.simran@yukawa.kyoto-u.ac.jp

† saiswagat009@gmail.com

‡ pksahoo@hyderabad.bits-pilani.ac.in

[20, 21]. In contrast to $f(R)$ gravity fourth-order field equations, $f(Q)$ gravity has second-order field equations unaffected by pathologies. Implementing a flat connection in the presence of affine coordinates, where all its components vanish, transforming covariant derivatives into partial derivatives, is a crucial feature of the $f(Q)$ theory. Thus, the $f(Q)$ approach can distinguish gravity and inertial effects. As a result, the formulation of the $f(Q)$ theory serves as a new basis for several modified theories of gravity.

Numerous investigations of modified $f(Q)$ models have been carried out extensively, varying from their use in cosmology and astrophysics to intriguing cosmic phenomenology at the background level [22–30]. Observational limits on the $f(Q)$ gravity have been made for many parameterizations of $f(Q)$ using different observational probes [31–36].

The role of dissipative processes in cosmology has been examined extensively in the literature. In particular, viscous effects, such as bulk and shear viscosity, can significantly influence the dynamical evolution of the Universe. To incorporate viscosity in the cosmic fluid, Eckart’s formalism is adopted, which provides a phenomenological description of the viscous dissipative processes arising when the system departs from local thermodynamic equilibrium [37]. Eckart’s approach has been widely employed in modeling late-time cosmic acceleration driven by viscous effects [38]. While Eckart’s formalism is known to suffer from causality issues, its mathematical simplicity has made it a widely used phenomenological framework and a natural starting point for cosmological applications. A more refined, causal description was later developed by Israel and Stewart through a second-order theory that introduces a finite relaxation time for dissipative processes [39]. Within this framework, bulk viscosity has been explored as an effective mechanism to account for dark-energy-like behavior in a variety of gravitational theories [40–46].

In the present work, we adopt Eckart’s first-order formalism to model bulk viscosity in the cosmic fluid. Within this framework, a bulk viscous fluid is characterized by the energy density ρ and an effective pressure $p_{eff} = p + \Pi$ where p denotes the equilibrium pressure and Π represents the bulk viscous pressure. For a homogeneous and isotropic Universe, Eckart’s theory yields $\Pi = -\zeta \vartheta$, ζ being the bulk viscosity coefficient and $\vartheta = 3H$ the expansion scalar, where $H = \frac{\dot{a}}{a}$ is the Hubble parameter. This formulation provides an effective description of dissipative effects at the background level and serves as the basis for our analysis in both general relativity and modified theories. We analyze the background evolution of a spatially flat Universe sourced by a bulk viscous fluid obeying the equation of state (EoS) $p = (\gamma - 1)\rho$, within the frameworks of general relativity and $f(Q)$ gravity. We examine the impact of varying γ on the cosmological dynamics and confront the resulting expansion histories with recent observational data, including observational Hubble measurements, Type Ia supernovae, and baryon acoustic oscillation data from DESI DR2. The free parameters of the model are constrained through a Markov Chain Monte Carlo (MCMC) analysis.

This paper is organized as follows. In section II, we present the basic ingredients of $f(Q)$ gravity. The Hubble parameter for viscous (in GR) and functional forms of $f(Q)$ is derived in section III by considering a flat universe with a bulk viscous fluid. Further, the constraints on the unknown model parameters are obtained using the observational data in section IV, followed by the results in section V. Section VI discusses the evolution of the deceleration, the EoS parameters, and the statefinder and Om diagnostics to distinguish dark energy models. Finally, section VII is devoted to summarizing the obtained results.

II. OVERVIEW OF $f(Q)$ GRAVITY

To explore the cosmological implications of symmetric teleparallel gravity, we consider the most general form of the affine connection, following [20, 47]

$$\tilde{\Gamma}^\alpha_{\mu\nu} = \hat{\Gamma}^\alpha_{\mu\nu} + K^\alpha_{\mu\nu} + L^\alpha_{\mu\nu}, \quad (1)$$

where the Levi-Civita connection of the metric $g_{\mu\nu}$, the contortion tensor, and disformation tensor are

$$\hat{\Gamma}^\alpha_{\mu\nu} = \frac{1}{2}g^{\alpha\sigma} \left(\partial_\mu g_{\sigma\nu} + \partial_\nu g_{\sigma\mu} - \partial_\sigma g_{\mu\nu} \right), \quad (2)$$

$$K^\alpha_{\mu\nu} = \frac{1}{2}g^{\alpha\sigma} \left(-T_{\mu\sigma\nu} - T_{\nu\sigma\mu} + T_{\sigma\mu\nu} \right), \quad (3)$$

$$L^\alpha_{\mu\nu} = \frac{1}{2}g^{\alpha\sigma} \left(-Q_{\mu\sigma\nu} - Q_{\nu\sigma\mu} + Q_{\sigma\mu\nu} \right). \quad (4)$$

Here, the torsion and nonmetricity tensors are defined by

$$\begin{aligned} T_{\mu\nu}^{\alpha} &= \tilde{\Gamma}_{\mu\nu}^{\alpha} - \tilde{\Gamma}_{\nu\mu}^{\alpha}, \\ Q_{\alpha\mu\nu} &= \Delta_{\alpha}g_{\mu\nu} = \partial_{\alpha}g_{\mu\nu} - \tilde{\Gamma}_{\mu\alpha}^{\lambda}g_{\lambda\nu} - \tilde{\Gamma}_{\nu\alpha}^{\lambda}g_{\mu\lambda}. \end{aligned}$$

Thus, the nonmetricity scalar is constructed as

$$Q = -g^{\mu\nu} \left(L_{\beta\mu}^{\alpha} L_{\nu\alpha}^{\beta} - L_{\beta\alpha}^{\alpha} L_{\mu\nu}^{\beta} \right). \quad (5)$$

Imposing the condition of symmetric teleparallelism renders the most general affine connection purely inertial. In this case, the connection can be written as

$$\tilde{\Gamma}_{\mu\nu}^{\alpha} = \frac{\partial x^{\alpha}}{\partial \zeta^{\sigma}} \frac{\partial^2 \zeta^{\sigma}}{\partial x^{\mu} \partial x^{\nu}},$$

where ζ^{σ} denotes an arbitrary function of the spacetime coordinates. By performing an appropriate general coordinate transformation, one may always choose $x^{\alpha} = \zeta^{\sigma}$, in which case the affine connection vanishes identically, $\tilde{\Gamma}_{\mu\nu}^{\alpha} = 0$. This special choice of coordinates is known as the coincident gauge [34, 48, 49]. In the coincident gauge, the nonmetricity tensor reduces to $Q_{\alpha\mu\nu} = \partial_{\alpha}g_{\mu\nu}$, implying that covariant derivatives coincide with ordinary partial derivatives. As a consequence, within symmetric teleparallel geometry, the dynamics of the Einstein-Hilbert theory are exactly recovered from the nonmetricity-based Lagrangian $2\mathcal{L} = Q$.

We now extend symmetric teleparallel gravity by promoting the nonmetricity scalar Q to an arbitrary function $f(Q)$. The corresponding action is given by

$$S = \int \left[-\frac{1}{2}f(Q) + L_m \right] \sqrt{-g} d^4x, \quad (6)$$

where L_m denotes the matter Lagrangian, g is the determinant of the metric $g_{\mu\nu}$, and $f(Q)$ is a general function of the nonmetricity scalar. In addition, the two independent traces of the nonmetricity tensor and the nonmetricity scalar are defined as $Q_{\alpha} = g^{\mu\nu} Q_{\alpha\mu\nu}$, $\tilde{Q}_{\alpha} = g^{\mu\nu} Q_{\mu\alpha\nu}$ and $Q = -Q_{\alpha\mu\nu} P^{\alpha\mu\nu}$. The latter expression includes the nonmetricity conjugate

$$P_{\mu\nu}^{\alpha} = -\frac{1}{2}L_{\mu\nu}^{\alpha} + \frac{1}{4}(Q^{\alpha} - \tilde{Q}^{\alpha})g_{\mu\nu} - \frac{1}{4}\delta^{\alpha}_{(\mu}\tilde{Q}_{\nu)}. \quad (7)$$

Varying the action with respect to the metric and connection, respectively, we obtain the field equations of $f(Q)$ gravity

$$\frac{2}{\sqrt{-g}} \nabla_{\alpha} (\sqrt{-g} f_Q P^{\alpha}_{\mu\nu}) + \frac{1}{2} g_{\mu\nu} f + f_Q (P_{\mu\alpha\beta} Q_{\nu}^{\alpha\beta} - 2Q_{\alpha\beta\mu} P^{\alpha\beta}_{\nu}) = T_{\mu\nu}, \quad (8)$$

where $f_Q = \frac{df}{dQ}$. Here, $T_{\mu\nu}$ is the stress-energy momentum tensor given by

$$T_{\mu\nu} = -\frac{2}{\sqrt{-g}} \frac{\delta(\sqrt{-g} L_m)}{\delta g^{\mu\nu}}. \quad (9)$$

The connection equation of motion can be derived by noting that the variation of the affine connection with respect to ζ^{α} is equivalent to an infinitesimal diffeomorphism. Consequently, one finds $\partial_{\zeta} \tilde{\Gamma}_{\mu\nu}^{\alpha} = -\mathcal{L}_{\zeta} \tilde{\Gamma}_{\mu\nu}^{\alpha} = -\nabla_{\mu} \nabla_{\nu} \zeta^{\alpha}$ [22, 50], where \mathcal{L}_{ζ} denotes the Lie derivative. Furthermore, in the absence of hypermomentum, the field equations for the connection follow directly from varying the action (6) with respect to the connection

$$\nabla_{\mu} \nabla_{\nu} \left(\sqrt{-g} f_Q P^{\mu\nu}_{\alpha} \right) = 0.$$

III. COSMOLOGICAL FORMULATION

We start with the Friedmann-Lemaître-Robertson-Walker (FLRW) metric in a homogeneous and isotropic flat spacetime

$$ds^2 = -dt^2 + a^2(t)\delta_{ij}dx^i dx^j, \quad (10)$$

where $a(t)$ is the scale factor of the universe. The nonmetricity reduces to $Q = 6H^2$.

Focusing our attention on the coincidence gauge, we can write the modified Friedman equations as

$$6f_Q H^2 - \frac{1}{2}f = \rho, \quad (11)$$

$$(12H^2 f_{QQ} + f_Q)\dot{H} = -\frac{1}{2}(\rho + p), \quad (12)$$

where $f_Q = \frac{df(Q)}{dQ}$, $f_{QQ} = \frac{d^2f(Q)}{dQ^2}$. Here, ρ and p are the energy density and pressure of the matter sector, respectively.

The idea of a stiff fluid with EoS $p = \rho$, originally proposed by Zel'dovich, has long served as a useful theoretical benchmark in cosmology. This component dilutes rapidly ($\rho \propto a^{-6}$) and therefore does not affect late-time evolution in its standard non-viscous form. However, when bulk viscosity is included, the effective pressure can deviate significantly from the ideal stiff limit, modifying the cosmic dynamics in a nontrivial manner [51–53]. This generalized viscous extension provides a broader phenomenological framework that interpolates between stiff, dust-like, and accelerated regimes, thereby motivating the study of viscous cosmologies within both GR and modified gravity scenarios.

In this context, it is convenient to consider a generalized barotropic EoS of the form

$$p = (\gamma - 1)\rho. \quad (13)$$

Here, $\gamma = 1$ corresponds to pressureless dust and $\gamma = 2$ reproduces the Zel'dovich stiff-fluid limit. The presence of bulk viscosity modifies the effective pressure, which can be written as

$$p' = p - 3\zeta H, \quad (14)$$

where ζ denotes the bulk viscosity coefficient. The energy-momentum conservation equation for the viscous fluid then takes the form

$$\dot{\rho} + 3H(\rho + p') = 0. \quad (15)$$

A. Viscous fluid dominated universe

Before turning to the effects of the $f(Q)$ formulation of gravity with the EoS given in Eq. (13), it is instructive to first examine the dynamics of the universe dominated solely by a viscous fluid. In this case, the Friedmann equation reduces to $3H^2 = \rho$, but, owing to the generalized EoS and the presence of bulk viscosity, the effective pressure is given by Eq. (14). Substituting this expression into the conservation Eq. (15), one finds that the cosmic expansion is governed by a modified evolution equation for the Hubble parameter,

$$\frac{dH}{dN} = -\frac{3}{2}(\zeta - \gamma H), \quad (16)$$

which admits the exact solution

$$H(z) = \frac{H_0 \tilde{\zeta}}{3\gamma} \left[1 - (1+z)^{3\gamma/2} \right] + H_0 (1+z)^{3\gamma/2}, \quad (17)$$

where we have introduced the dimensionless viscosity parameter $\tilde{\zeta} \equiv \frac{3\zeta}{H_0}$. In the dust limit ($\gamma = 1$) and in the absence of viscosity ($\tilde{\zeta} = 0$), the standard matter-dominated expansion is recovered. Allowing for nonzero viscosity, however, leads to a much richer cosmological behavior. In particular, the case $\gamma = 1$ with non-zero viscosity was

studied in detail [54], where it was shown that bulk viscous pressure can effectively drive the late-time accelerated expansion of the universe. Since the cosmic dynamics are entirely governed by the viscous fluid in this scenario, the expansion history is fully determined by the parameters. It could be found that the limit $0 < \tilde{\zeta} \leq 3$ always allows for a de-Sitter state in the far future. Now, the viscous case where $\gamma = 2$, corresponding to a Zel'dovich fluid, was investigated in [55, 56]. While the non-viscous case will simply correspond to a stiff fluid behavior, the presence of effective pressure, as in Eq. (14), allows the existence of an accelerating late-time solution in [56]. For completeness, we shall present updated constraints for the more general case, in which γ is free to vary, in the range $0 < \gamma \leq 2$.

B. Viscous $f(Q)$ formalism

In this section, we start our analysis using the exponential model investigated in [57–61], which tends to the Λ CDM paradigm at high redshifts while producing a non-negligible impact in low- z cosmology. The $f(Q)$ function is given by

$$f(Q) = Qe^{\alpha Q_0/Q}, \quad (18)$$

with α being a dimensionless constant, while $Q_0 = 6H_0^2$. Moreover, since the model tends to the GR limit at early times ($Q > Q_0$), it satisfies the BBN constraints. Note that the model effectively simplifies to the polynomial case at some point in cosmic history as Q_0/Q declines. This model behaves like an endless variety of models coexisting, with one acting dominantly at each point in cosmic history.

The energy density of the fluid, denoted hereafter by ρ_f , can be obtained from Eq. (11) and takes the form

$$\rho_f = 3H_0^2 e^{\alpha/E^2} (E^2 - 2\alpha), \quad (19)$$

where we have introduced the dimensionless Hubble parameter $E \equiv H/H_0$. Identifying ρ_0 as the present energy density of the fluid leads to the following constraint at the present time

$$\alpha = \frac{1}{2} + \mathcal{W} \left(-\frac{\Omega_{f,0}}{2e^{1/2}} \right). \quad (20)$$

where $\mathcal{W}(x)$ is the Lambert function, and in principle, reduces the number of free parameters to the same one as of the viscous model in equation (17). In practice, this relation fixes the value of α once $\Omega_{f,0}$ is constrained. To determine the background evolution, we solve the equations of motion using Eq. (12) together with the effective pressure defined in (14). Throughout this analysis, we assume a barotropic EoS of the form $p = (\gamma - 1)\rho$, which reproduces the pressureless matter behavior for $\gamma = 1$. Eventually, one can derive the equation of the normalized Hubble function E as

$$E' = -\frac{3}{2} \frac{\left[\gamma e^{\alpha/E^2} (E^2 - 2\alpha) - \tilde{\zeta} E \right]}{E e^{\alpha/E^2} \left[1 + \frac{\alpha}{E^2} \left(\frac{2\alpha}{E^2} - 1 \right) \right]}, \quad (21)$$

where we have defined $\tilde{\zeta} = \frac{3\zeta}{H_0}$ and a prime denotes a derivative with respect to $N = \ln a$. Due to the nonlinear structure introduced by the exponential $f(Q)$ function and the viscous contribution, this equation does not admit a closed-form analytical solution and is therefore solved numerically. Initial conditions are imposed at the present epoch, $E(z=0) = 1$, and the resulting evolution is used to reconstruct the background expansion history.

IV. COSMOLOGICAL CONSTRAINTS

The next step of our analysis is to constrain the proposed models using observational data. To this end, we perform a MCMC analysis employing a combination of independent cosmological probes, including cosmic chronometers (CC), baryon acoustic oscillation measurements from DESI DR2, gamma-ray bursts (GRBs), and the Union3 Type Ia supernova compilation.

The parameter estimation is carried out using the publicly available Python package `emcee` [62], which implements an affine-invariant ensemble sampler well suited for exploring multidimensional parameter spaces. The resulting posterior distributions are subsequently analyzed and visualized using the `GetDist` package [63], allowing for the computation of marginalized constraints, confidence intervals, and joint contour plots. In the following, we provide a detailed description of the observational datasets and outline the methodology adopted for likelihood construction and parameter inference.

A. Cosmic Chronometers (CC)

The CC dataset is one of the most developed observational datasets that tests various cosmological models and is derived using the so-called differential age of the galaxies described in [64, 65]. With the method mentioned above, one could derive the Hubble parameter value at a particular redshift with the following formula

$$H(z) = \frac{-1}{1+z} \frac{dz}{dt}.$$

One could derive the ratio using the equation dz/dt as $\Delta z/\Delta t$, where Δz can be thought of as the separation of a redshift in a dataset, values of which could be easily derived from the high-resolution spectroscopy. On the other hand, the derivation of Δt is rather complex and challenging. Δt usually could be derived from old stellar populations that endanger most galaxies up to very high redshifts.

The data points considered in this study are collected from the Refs. [66–69]. The methodology for constructing the χ^2 function is discussed in detail in Ref. [70], and the full covariance matrix corresponding to the correlated CC dataset is taken from Ref. [71].

B. DESI BAO DR2

This data set consists of Baryon Acoustic Oscillation (BAO) measurements from the Dark Energy Spectroscopic Instrument (DESI) Data Release II [8], which extends and improves upon the earlier DR1 results [7, 72]. The key observables are the ratios $\{D_M/r_d, D_H/r_d, D_V/r_d\}$, where D_M is the comoving angular diameter distance, D_H the Hubble distance, D_V the spherically averaged BAO distance, and r_d the comoving sound horizon at the drag epoch [7, 73]. In recent years, such datasets have revealed intriguing hints that dark energy may evolve over time, challenging the standard Λ CDM model [74–78]. A detailed description of DESI DR2 and the formulation of χ^2 is presented in the Ref. [79].

C. Gamma-ray bursts (GRBs)

We investigate the empirical correlation between the observed photon energy at the peak of the spectral flux, $E_{p,i}$, corresponding to the maximum of the νF_ν spectrum, and the isotropic equivalent radiated energy, E_{iso} . This relation is commonly expressed as [80]

$$\log\left(\frac{E_{\text{iso}}}{1 \text{ erg}}\right) = a + b \log\left(\frac{E_{p,i}}{300 \text{ keV}}\right), \quad (22)$$

where a and b are calibration constants.

The quantity $E_{p,i}$ denotes the spectral peak energy in the GRB rest frame and is related to the observer-frame peak energy E_p via

$$E_{p,i} = E_p(1+z), \quad (23)$$

with z being the source redshift. This correlation provides valuable constraints on prompt-emission models of gamma-ray bursts (GRBs) and, importantly, suggests that GRBs can be used as distance indicators.

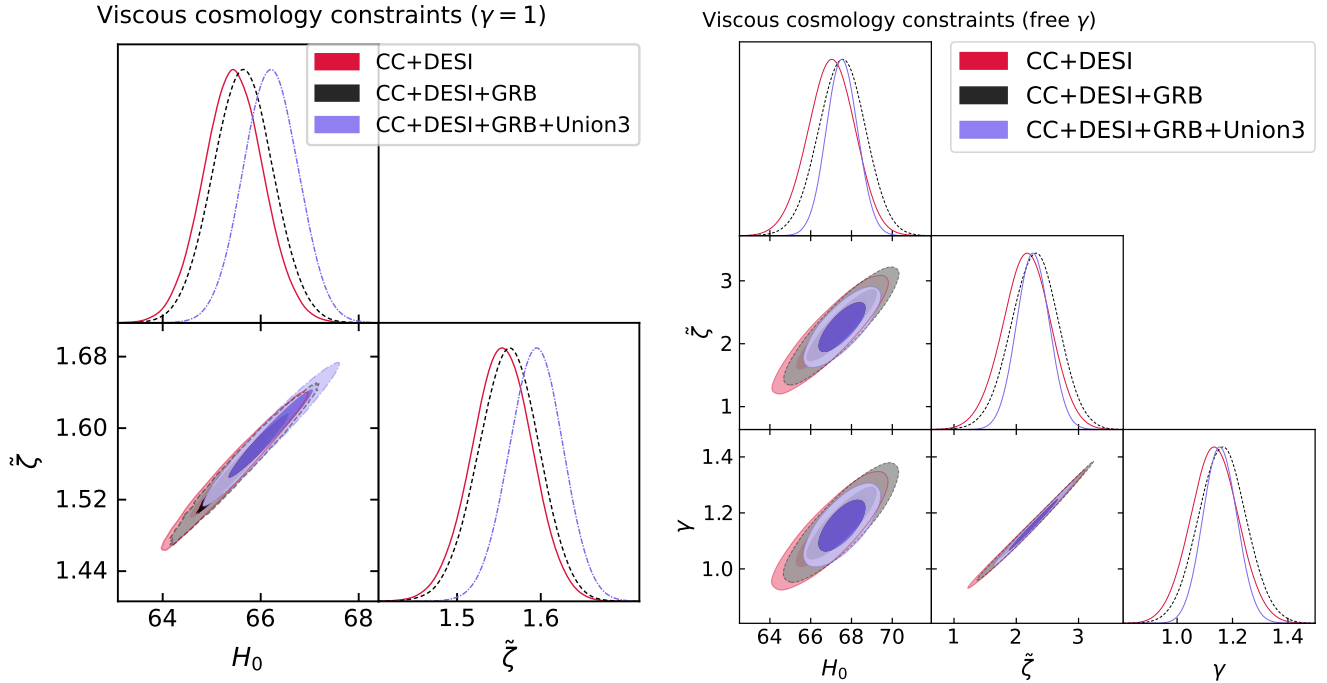


FIG. 1: The 1σ and 2σ likelihood contours for the bulk viscous model, for $\gamma = 1$ and free γ .

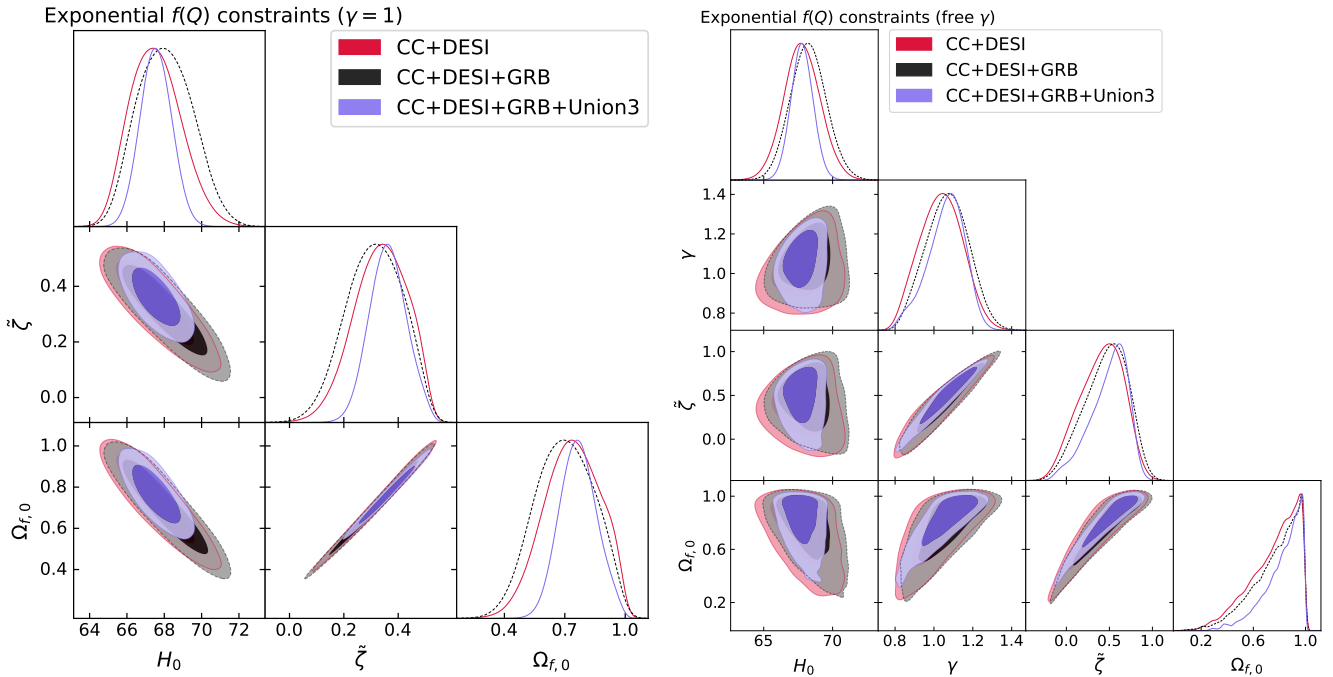


FIG. 2: The 1σ and 2σ likelihood contours for the viscous exponential $f(Q)$ model, for $\gamma = 1$ and free γ .

The isotropic-equivalent energy is derived from the bolometric fluence S_{bolo} according to

$$E_{\text{iso}} = 4\pi d_L^2(z, \mathbf{c}_p) S_{\text{bolo}} (1+z)^{-1}, \quad (24)$$

where d_L is the luminosity distance and \mathbf{c}_p denotes the set of cosmological parameters defining the background model.

To ensure the reliability of GRBs as standardizable candles, a consistent calibration of the above correlation is essential. We analyze a sample of 162 long GRBs compiled from updated spectral and intensity measurements [81, 82]. The redshift range of the sample spans $0.03 \leq z \leq 9.3$, significantly extending beyond that of Type Ia supernovae. All selected events have securely measured redshifts and rest-frame peak energies. Most of the data originate from joint observations by *Swift*/BAT and *Fermi*/GBM or *Konus-Wind*, with a small number of cases where $E_{p,i}$ is directly determined from *Swift*/BAT within the 15–150 keV band. For GRBs detected by multiple instruments, the reported uncertainties in $E_{p,i}$ and E_{iso} consistently incorporate the measurements and associated errors from each detector.

The χ^2 function is defined as

$$\chi_{GRBs}^2(\theta) = \sum_{i=1}^{\mathcal{N}} \left(\frac{\mu_{\text{obs}}(z_i) - \mu_{\text{th}}(z_i, \theta)}{\sigma_i} \right)^2, \quad (25)$$

where θ is the parameter space and \mathcal{N} is the sample size of GRBs.

D. Union 3

The Union3 supernova compilation comprises 2087 Type Ia supernovae drawn from 24 independent data samples, spanning a redshift range of $0.01 \leq z \leq 2.26$. All supernovae are standardized onto a common distance scale using the SALT3 light-curve fitting method. The full dataset is analyzed and binned within the UNITY1.5 Bayesian statistical framework, resulting in a set of 22 binned distance-modulus measurements used in this analysis [83].

One of the key advances of the Union3 compilation lies in its rigorous treatment of systematic uncertainties. In contrast to earlier supernova data sets that relied primarily on statistical errors, Union3 provides a full covariance matrix \mathbf{C} that consistently incorporates both statistical and systematic contributions,

$$\mathbf{C}_{\text{union}} = \mathbf{D}_{\text{stat}} + \mathbf{C}_{\text{sys}}. \quad (26)$$

The statistical component \mathbf{D}_{stat} includes measurement noise, photometric uncertainties, and intrinsic dispersion, while the systematic covariance \mathbf{C}_{sys} accounts for uncertainties associated with photometric calibration (including zeropoints and filter transmission functions), host-galaxy corrections, dust extinction laws, light-curve model uncertainties, and peculiar velocity effects.

These systematic uncertainties are propagated through the SALT2 light-curve fitting and cosmological analysis pipeline using Monte Carlo simulations, ensuring a consistent treatment of correlated errors across the full supernova sample. Cosmological constraints are obtained by comparing the observed distance moduli μ_{obs} with the theoretical predictions $\mu_{\text{model}}(z, \theta)$. The goodness of fit is quantified using the standard chi-squared statistic,

$$\chi^2 = (\mu_{\text{obs}} - \mu_{\text{model}})^T \mathbf{C}_{\text{union}}^{-1} (\mu_{\text{obs}} - \mu_{\text{model}}). \quad (27)$$

The full covariance matrix $\mathbf{C}_{\text{union}}$ is taken from Ref. [83].

V. RESULTS

With the necessary tools and methodology in place, we are now in a position to perform the observational analysis of the gravity model. In what follows, we implement the framework outlined in the previous section and carry out a comprehensive parameter inference using different combinations of the available datasets. The combinations we considered are CC+DESI, CC+DESI+GRB, and CC+DESI+GRB+Union3.

The resulting marginalized constraints and best-fit values are summarized in Table I. We consider both the dust case ($\gamma = 1$) and the free- γ scenario within the viscous GR and viscous $f(Q)$ frameworks. Figures 1 and 2 display the corresponding one- and two-dimensional posterior distributions for the different dataset combinations.

In the bulk viscous model, the contours reveal a clear positive correlation between H_0 and $\tilde{\zeta}$, indicating that larger viscous contributions are associated with higher preferred expansion rates. This reflects the role of viscous pressure in directly contributing to late-time acceleration. When γ is allowed to vary, the best-fit region shifts moderately

TABLE I: Best-fit values and constraints for the viscous-dominated and viscous exponential $f(Q)$ models obtained from different combinations of observational datasets.

Model	Ω_f	H_0 [km s $^{-1}$ Mpc $^{-1}$]	$\tilde{\zeta}$	γ	q_0	$w_{eff,0}$
CC + DESI						
Viscous ($\gamma = 1$)	–	65.46 ± 0.62	1.554 ± 0.037	1	$-0.27^{+0.018}_{-0.017}$	$-0.52^{+0.012}_{-0.011}$
Viscous (free γ)	–	67.0 ± 1.2	2.17 ± 0.40	1.137 ± 0.089	$-0.38^{+0.064}_{-0.062}$	$-0.58^{+0.043}_{-0.041}$
$f(Q)$ ($\gamma = 1$)	0.73 ± 0.14	$67.6^{+1.3}_{-1.6}$	$0.33^{+0.11}_{-0.091}$	1	$-0.46^{+0.105}_{-0.092}$	$-0.64^{+0.070}_{-0.061}$
$f(Q)$ (free γ)	$0.754^{+0.24}_{-0.081}$	67.8 ± 1.3	$0.40^{+0.29}_{-0.22}$	1.04 ± 0.12	$-0.45^{+0.079}_{-0.090}$	$-0.63^{+0.053}_{-0.060}$
CC + DESI + GRB						
Viscous ($\gamma = 1$)	–	65.64 ± 0.62	1.561 ± 0.036	1	$-0.28^{+0.018}_{-0.018}$	$-0.52^{+0.012}_{-0.012}$
Viscous (free γ)	–	67.5 ± 1.2	2.29 ± 0.38	1.161 ± 0.087	$-0.41^{+0.063}_{-0.060}$	$-0.60^{+0.042}_{-0.040}$
$f(Q)$ ($\gamma = 1$)	0.70 ± 0.14	$68.1^{+1.3}_{-1.5}$	0.31 ± 0.10	1	$-0.47^{+0.104}_{-0.086}$	$-0.65^{+0.069}_{-0.057}$
$f(Q)$ (free γ)	$0.764^{+0.23}_{-0.071}$	68.3 ± 1.3	$0.45^{+0.31}_{-0.21}$	1.06 ± 0.11	$-0.47^{+0.084}_{-0.081}$	$-0.65^{+0.056}_{-0.054}$
CC + DESI + GRB + Union3						
Viscous ($\gamma = 1$)	–	66.21 ± 0.57	1.594 ± 0.032	1	$-0.29^{+0.016}_{-0.016}$	$-0.53^{+0.010}_{-0.010}$
Viscous (free γ)	–	67.55 ± 0.77	2.27 ± 0.26	1.156 ± 0.061	$-0.41^{+0.039}_{-0.040}$	$-0.60^{+0.026}_{-0.027}$
$f(Q)$ ($\gamma = 1$)	$0.765^{+0.090}_{-0.10}$	67.57 ± 0.83	0.361 ± 0.070	1	$-0.44^{+0.066}_{-0.056}$	$-0.62^{+0.044}_{-0.037}$
$f(Q)$ (free γ)	$0.837^{+0.16}_{-0.048}$	67.75 ± 0.80	$0.51^{+0.24}_{-0.15}$	$1.07^{+0.10}_{-0.078}$	$-0.43^{+0.051}_{-0.043}$	$-0.62^{+0.034}_{-0.029}$

and an additional correlation between γ and $\tilde{\zeta}$ emerges, while the overall correlation structure between H_0 and the viscous sector remains robust. This indicates that both dissipative effects and the effective matter equation of state jointly influence the expansion dynamics.

For the viscous $f(Q)$ model, the contour structure differs qualitatively. A pronounced negative correlation is observed between $\Omega_{f,0}$ and $\tilde{\zeta}$, demonstrating that the modified-gravity contribution and viscous effects compensate each other in driving late-time expansion. A stronger nonmetricity contribution corresponds to a smaller required viscous term, evidencing a genuine interplay between geometry and dissipation rather than the dominance of a single mechanism. In the $(\Omega_{f,0}, \tilde{\zeta})$ sector the allowed region is more tightly localized compared to the pure viscous case, particularly after inclusion of Union3 data. Allowing γ to vary broadens the contours but preserves the overall degeneracy structure, with $\Omega_{f,0}$ consistently clustering around values comparable to the effective dark-energy fraction in Λ CDM.

Figure 3 shows the best-fit reconstructed expansion histories for the bulk viscous model (left panel) and the viscous $f(Q)$ model (right panel), plotted in terms of $H(z)/(1+z)$. This representation highlights departures from the standard Λ CDM behavior and allows for a direct comparison between different dynamical scenarios. Solid lines correspond to the dust case ($\gamma = 1$), dashed lines denote the free- γ case, and the dotted curve shows the Λ CDM prediction. Different colors indicate the dataset combinations used in the reconstruction.

In the bulk viscous model, the reconstructed histories follow the Λ CDM curve at low redshift and display moderate deviations around intermediate redshifts. Allowing γ to vary leads to small shifts in the reconstructed curves but preserves the overall shape and location of the minimum in $H(z)/(1+z)$, indicating that the late-time expansion is primarily governed by the viscous contribution. In the viscous $f(Q)$ model, the reconstructed expansion histories remain closer to the Λ CDM prediction over the full redshift range. The inclusion of the nonmetricity sector slightly modifies the location of the minimum and reduces the spread between different reconstructions as additional datasets are included. This behavior is consistent with the tighter parameter constraints obtained for the $f(Q)$ model and reflects its ability to reproduce a Λ CDM-like expansion history while retaining a dynamical origin for cosmic acceleration.

Figure 4 shows the reconstructed distance modulus $\mu(z)$ for the bulk viscous and viscous $f(Q)$ models, for both $\gamma = 1$ and free γ . In both cases, the reconstructions closely follow the Λ CDM prediction and are consistent with the GRBs and Union3 data over the full redshift range. Allowing γ to vary produces only small shifts in the curves without changing their overall behavior.

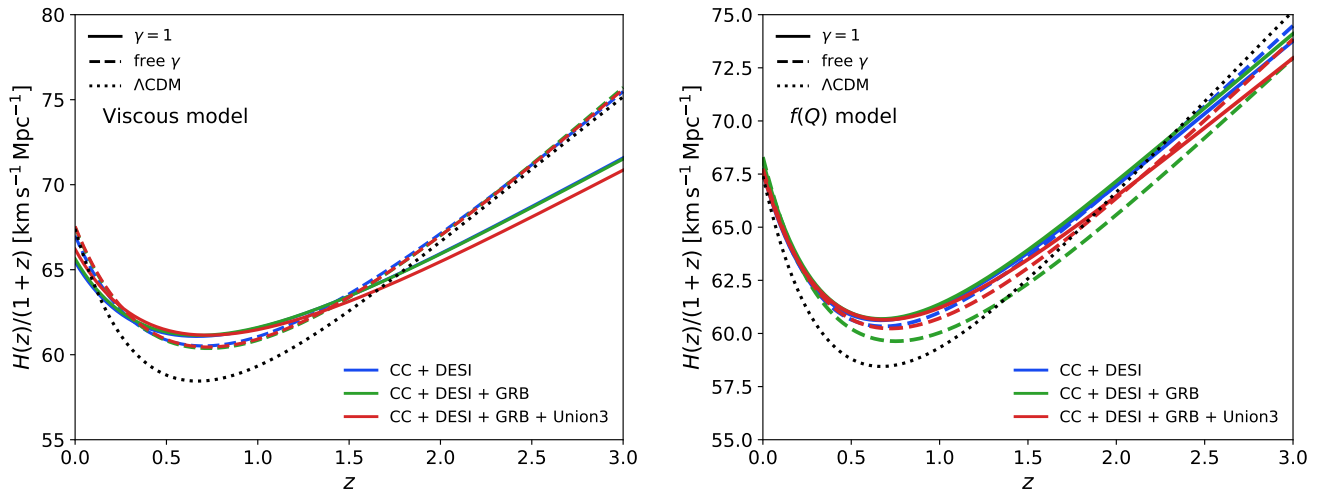


FIG. 3: Best-fit reconstructed expansion histories for the considered models. The panels show the predictions for $H(z)/(1+z)$ within each individual model, with best-fit parameters determined from different dataset combinations.

To assess the relative performance of the viscous and viscous $f(Q)$ models with respect to the standard cosmological scenario, we carry out a statistical comparison based on the minimum χ^2 , the Akaike Information Criterion (AIC), and the Bayesian Information Criterion (BIC). The Λ CDM model (also depicted in figure 11) is adopted as the reference owing to its well-established success in fitting a broad range of cosmological observations. While the minimum χ^2 provides a measure of the goodness of fit, the information criteria incorporate a penalty for the number of free parameters, thereby enabling a balanced comparison between fit quality and model complexity. The AIC and BIC are defined as $AIC = \chi^2_{\min} + 2d$ and $BIC = \chi^2_{\min} + d \ln N$, respectively, where d denotes the number of model parameters and N is the size of the dataset. The statistical preference of a given model is quantified through the differences ΔAIC and ΔBIC relative to Λ CDM. In general, $\Delta AIC \lesssim 2$ indicates strong support, $2 \lesssim \Delta AIC \lesssim 7$ suggests moderate support, and larger values imply no significant preference. The BIC provides a more conservative assessment, with $\Delta BIC < 2$ favoring a model, $2 \leq \Delta BIC < 6$ indicating moderate evidence, and $\Delta BIC > 6$ disfavoring the model relative to Λ CDM.

Table II presents a statistical comparison of the bulk viscous and viscous $f(Q)$ models relative to Λ CDM using the minimum χ^2 , AIC, and BIC. For the $CC + DESI$ dataset, both viscous and $f(Q)$ models provide improved fits compared to Λ CDM, particularly when the equation-of-state parameter γ is allowed to vary. Although the information criteria account for the increased number of free parameters, the resulting AIC values remain competitive, indicating that the improvement in goodness of fit is not achieved at the expense of excessive model complexity. A similar behavior is observed when GRB data are included, where the viscous and viscous $f(Q)$ models continue to perform comparably to Λ CDM. For the full $CC + DESI + GRB + Union3$ dataset combination, both models yield a noticeably better fit in terms of χ^2_{\min} , with negative ΔAIC values pointing to a mild statistical preference. The BIC, being more conservative, shows a weaker preference but remains consistent with these extended scenarios. Overall, the information criteria support the conclusion that dynamical viscosity and modified gravity provide statistically viable and well-performing alternatives to Λ CDM within the current observational precision.

VI. COSMOLOGICAL PARAMETERS

To assess the physical viability of the cosmological models constructed in this work, it is useful to examine a set of diagnostic parameters characterizing the background dynamics. A primary quantity of interest is the deceleration parameter, defined as $q = -\frac{\ddot{H}}{H^2} - 1$, which directly quantifies the acceleration of the cosmic expansion. Positive values of q correspond to a decelerating Universe, whereas negative values signal an accelerated expansion.

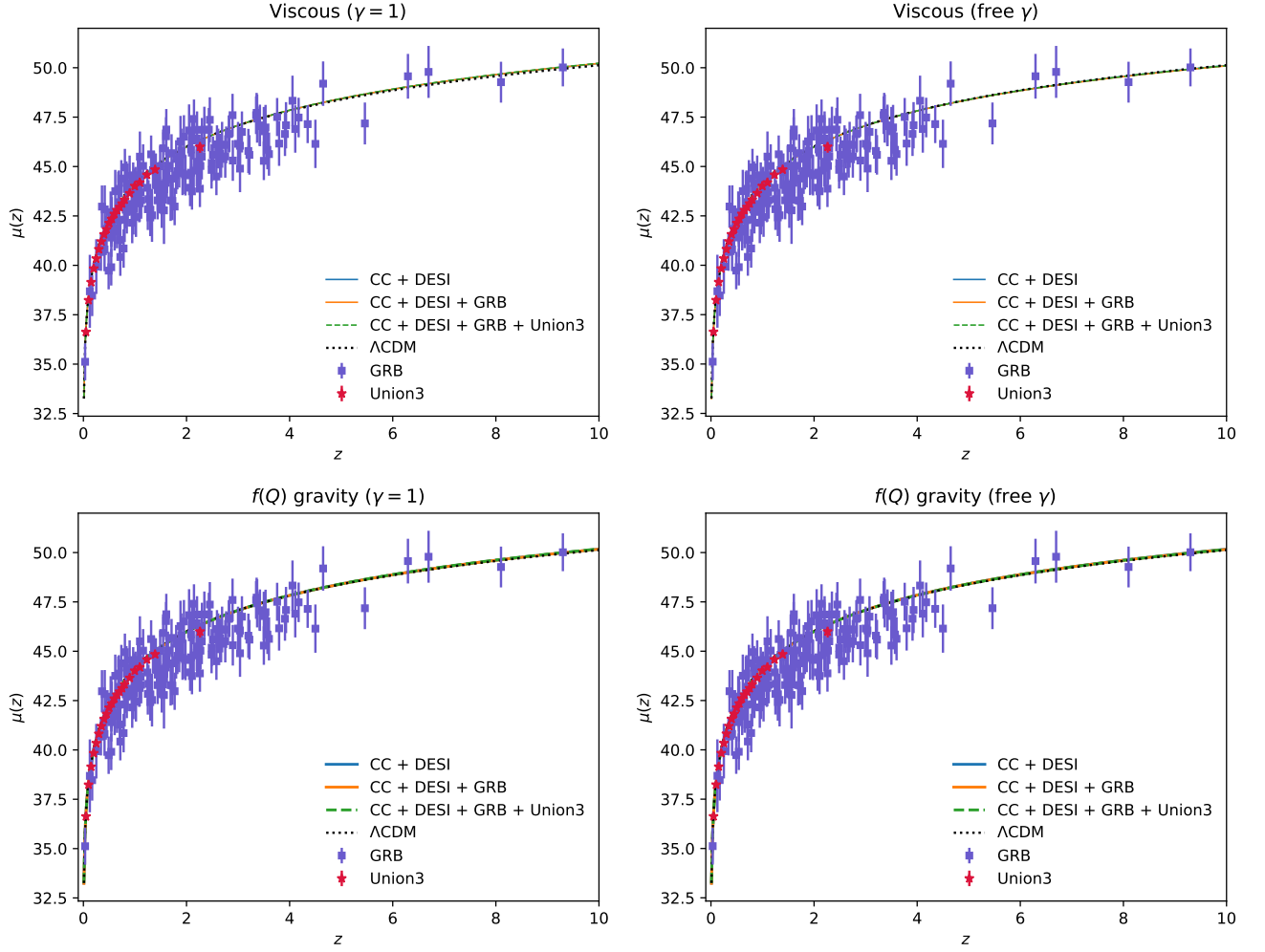


FIG. 4: Reconstructed distance modulus $\mu(z)$ for the viscous (upper panel) and exponential $f(Q)$ (lower panel) cosmological models. Solid curves denote the posterior mean predictions from different data combinations, with GRBs and Union3 data shown for reference.

Another key diagnostic is the effective EoS parameter, $w_{\text{eff}} = \frac{p'}{\rho}$. It is derived directly from the effective pressure and energy density introduced in the field equations beforehand. The effective EoS parameter provides a useful phenomenological description of the dominant cosmic component: $w_{\text{eff}} = 0$ corresponds to pressureless matter, $w_{\text{eff}} = 1/3$ for radiation era, $w_{\text{eff}} = -1$ for cosmological-constant-like behavior. There are more exotic forms of EoS, like the one with $w_{\text{eff}} < -1$ (phantom fluid), and $-1 < w_{\text{eff}} < -\frac{1}{3}$ as the quintessence phase.

Figures 5 and 6 show the reconstructed evolution of the deceleration parameter $q(z)$ and the effective EoS parameter obtained from different combinations of cosmological datasets. In all cases, the universe undergoes a smooth transition from a decelerating phase at high redshift to a late-time accelerating phase, with $q(z)$ changing sign around $z \sim 0.5 - 0.7$. The inclusion of additional datasets, in particular GRBs and the Union3 supernova compilation, significantly tightens the constraints at low redshift and leads to a more precise determination of the transition epoch. The EoS remains in a quintessence-like accelerating regime, while approaching matter-like behavior at higher redshifts [44, 84–86]. No evidence for phantom crossing is observed within the 1σ confidence region. The mean evolution curves and the corresponding confidence regions are obtained directly from the MCMC posterior samples, ensuring that the reconstructed histories fully reflect the underlying parameter correlations.

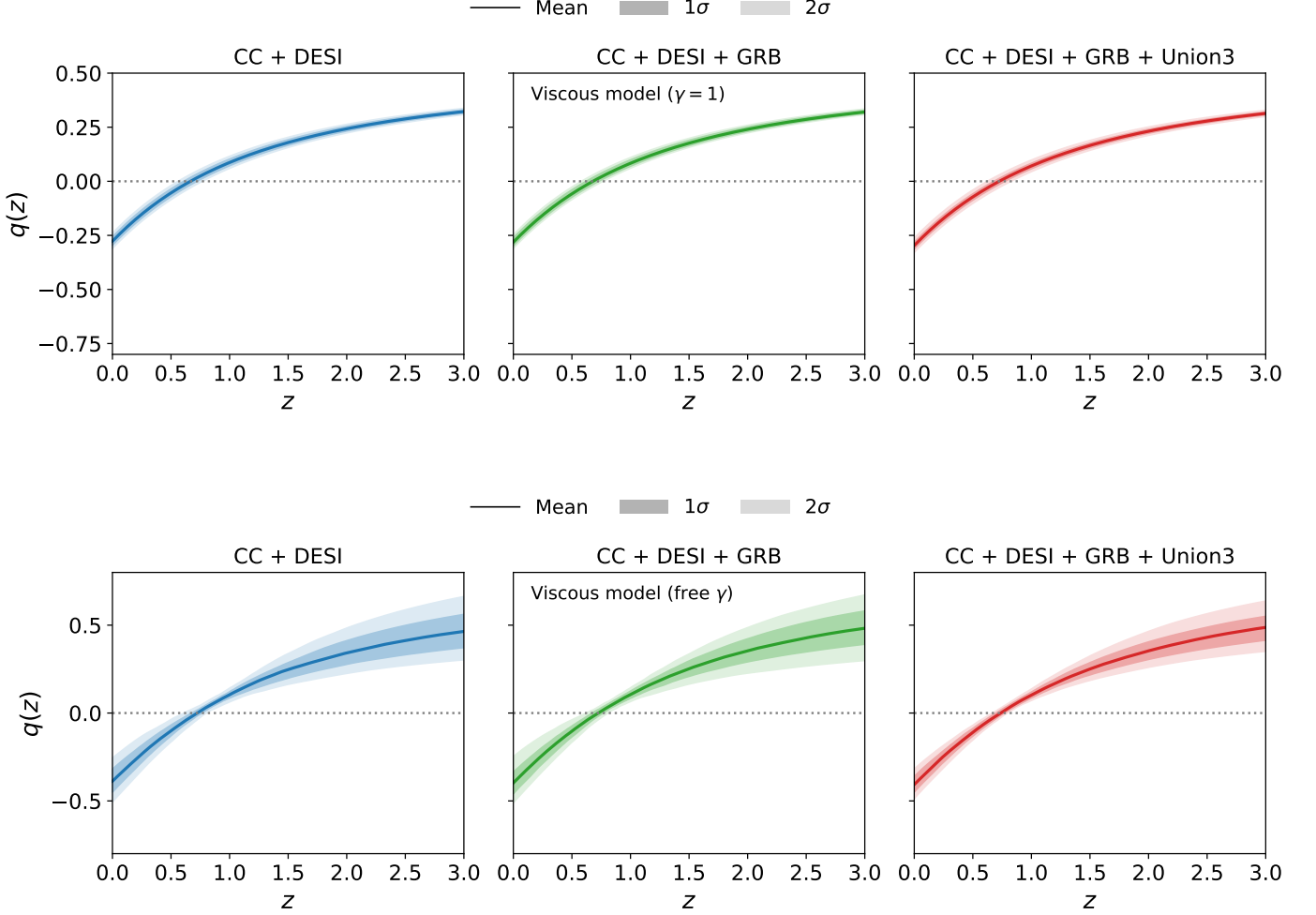


FIG. 5: Deceleration parameter for the viscous fluid model with $\gamma = 1$ and free γ , reconstructed from observational data. The 1σ and 2σ regions are obtained using posterior samples from the MCMC chains.

A. Statefinder and $\text{Om}(z)$ diagnostics

The statefinder diagnostics is a widely used practice to differentiate various cosmological models and track their evolution/phase transitions. For such a purpose, the statefinder pair was introduced in the literature [87, 88]

$$r = \frac{\ddot{a}}{aH^3}, \quad s = \frac{r-1}{3(q-1/2)}. \quad (28)$$

This pair, for the sake of simplicity, could be completely defined in terms of the deceleration parameter

$$r(z) = q(z)(1 + 2q(z)) + q'(z)(1 + z),$$

$$s(z) = \frac{r(z) - 1}{3(q(z) - 1/2)}.$$

In order to perform the aforementioned diagnostics, we need to construct parametric plots within the $r - s$ plane, for which different points and regions correspond to the different states of matter/stages of universe evolution: Λ CDM corresponds to $(s = 0, r = 1)$, Chaplygin Gas (CG) corresponds to $(s < 0, r > 1)$, and quintessence corresponds to $(s > 0, r < 1)$.

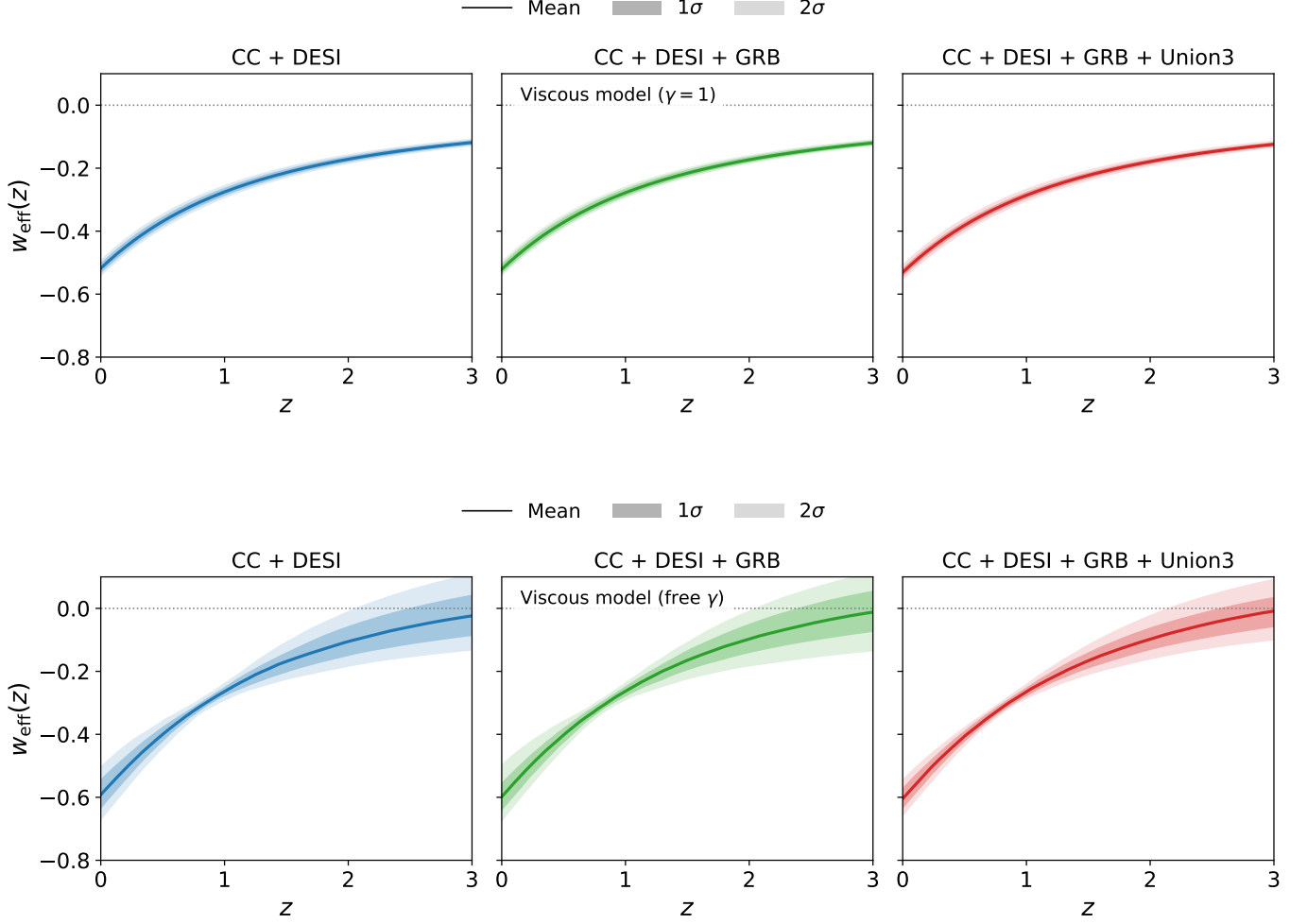


FIG. 6: Effective equation of state for the bulk viscous fluid model with $\gamma = 1$ and free γ , reconstructed from observational data. The confidence regions are obtained using posterior samples from the MCMC chains.

We now turn to a discussion of the well-known and widely used $Om(z)$ diagnostics. This diagnostic was first introduced in [89, 90], where $Om(z)$ is defined as

$$Om(z) = \frac{E^2(z) - 1}{(1+z)^3 - 1}. \quad (29)$$

Figures 9 and 10 summarize the geometrical diagnostics of the viscous cosmological models through the statefinder parameters (r, s) and (r, q) , together with the $Om(z)$ diagnostic, for the different combinations of observational datasets. In the r - s plane, the reconstructed trajectories pass close to the Λ CDM fixed point $(r, s) = (1, 0)$ at late times and then gradually evolve into the quintessence region as the redshift increases. Importantly, the evolution remains well separated from the Chaplygin gas sector, indicating that the accelerated expansion in these models is not driven by an exotic unified dark-fluid behavior but instead by an effective quintessence-like dynamics induced by viscosity and modified gravity effects. A similar picture emerges in the r - q plane, where the trajectories clearly trace a smooth transition from a decelerated to an accelerated expansion phase, with controlled deviations from the Λ CDM limit.

The $Om(z)$ diagnostic further supports this interpretation. While Λ CDM predicts a constant $Om(z)$, the viscous models exhibit a mild redshift dependence, reflecting the dynamical nature of the effective dark-energy sector. At

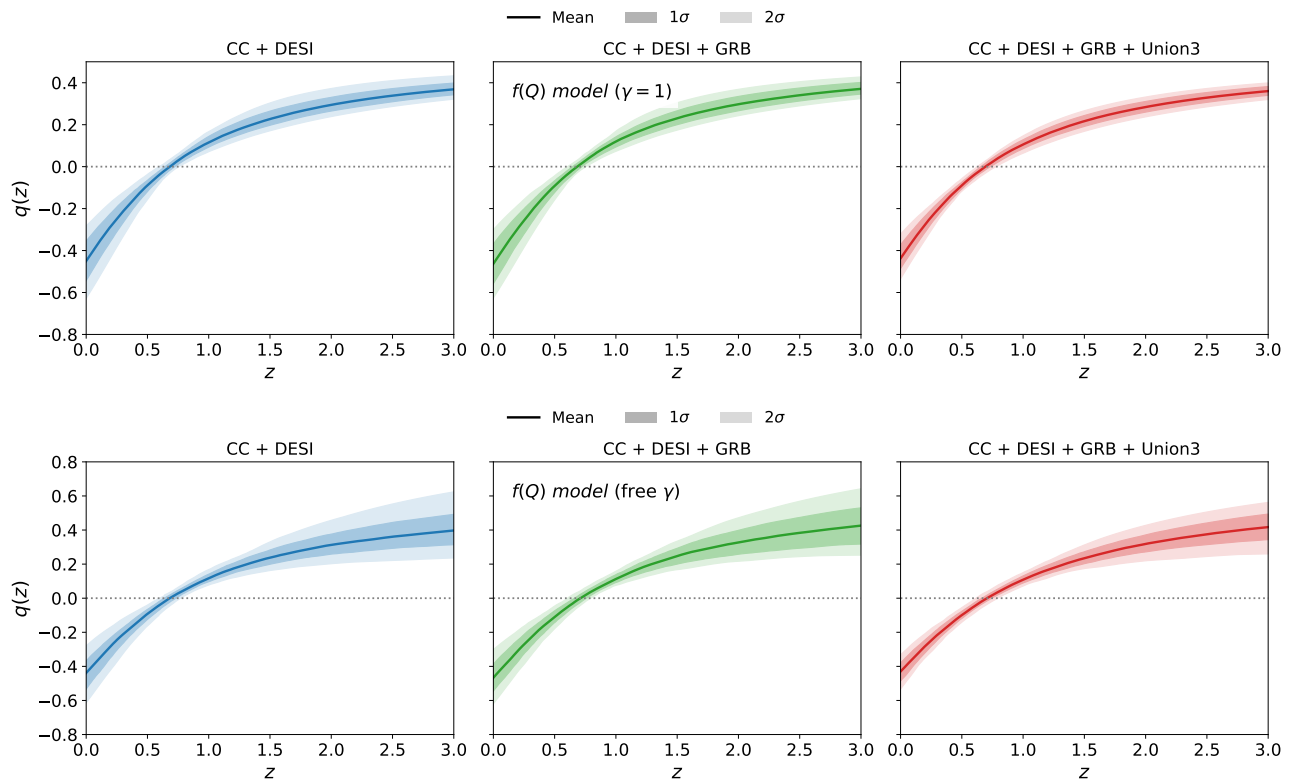


FIG. 7: Deceleration parameter for the viscous fluid model within the $f(Q)$ framework, shown for both fixed $\gamma = 1$ and free- γ cases. The 1σ and 2σ confidence regions are reconstructed using posterior samples from the MCMC chains.

low redshift, the reconstructed $Om(z)$ curves remain compatible with observational bounds, whereas at higher redshifts they gradually approach matter-dominated behavior. Allowing the equation-of-state parameter γ to vary slightly modifies the detailed shape of the trajectories but does not change their overall qualitative behavior. Moreover, the inclusion of GRBs and Union3 data leads to visibly tighter constraints, underscoring the role of complementary low- and high-redshift probes in sharpening the reconstruction. Overall, these geometrical diagnostics consistently show that the viscous $f(Q)$ framework provides a stable and physically plausible description of late-time cosmic acceleration, while maintaining a close connection to the Λ CDM paradigm.

VII. CONCLUSIONS

Motivated by the extended symmetric teleparallel equivalent of General Relativity, we investigated the cosmological evolution of the Universe in the presence of a bulk viscous fluid within the exponential $f(Q)$ gravity framework. We considered both fixed $\gamma = 1$ and free γ scenarios, adopting the generalized form $f(Q) = Qe^{\alpha Q_0/Q}$, where α is the model parameter. This form is well motivated and reduces to the Λ CDM paradigm at high redshifts, while allowing nontrivial deviations at late times [28, 35].

We performed a Bayesian MCMC analysis for two classes of models: a viscous fluid in General Relativity and a viscous fluid embedded in exponential $f(Q)$ gravity. The models were constrained using cosmic chronometers, DESI DR2 BAO measurements, and Type Ia supernova data (GRBs and Union3). The resulting best-fit values and 1σ constraints are presented in Table I. The parameter constraints remain stable across dataset combinations, with mild tightening when GRBs and Union3 data are included. The Hubble parameter is consistently constrained within $H_0 \sim 65\text{--}68 \text{ km s}^{-1} \text{ Mpc}^{-1}$, with the $f(Q)$ model generally favoring slightly higher values than the viscous scenario. These values remain compatible with Planck measurements while lying below local distance-ladder measurements,

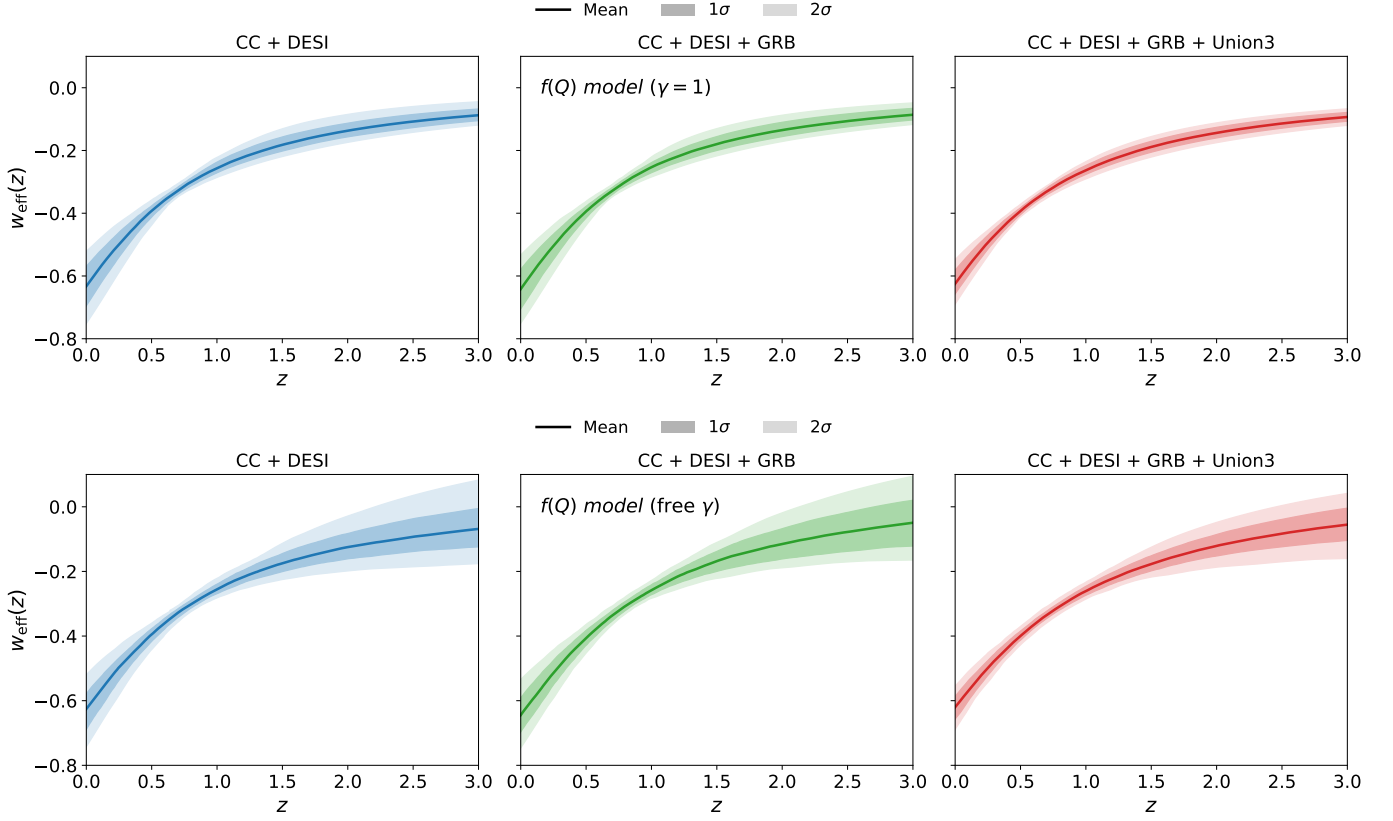


FIG. 8: Effective equation of state for the bulk viscous fluid within the $f(Q)$ framework, shown for both fixed $\gamma = 1$ and free- γ cases. The 1σ and 2σ confidence regions are reconstructed using posterior samples from the MCMC chains.

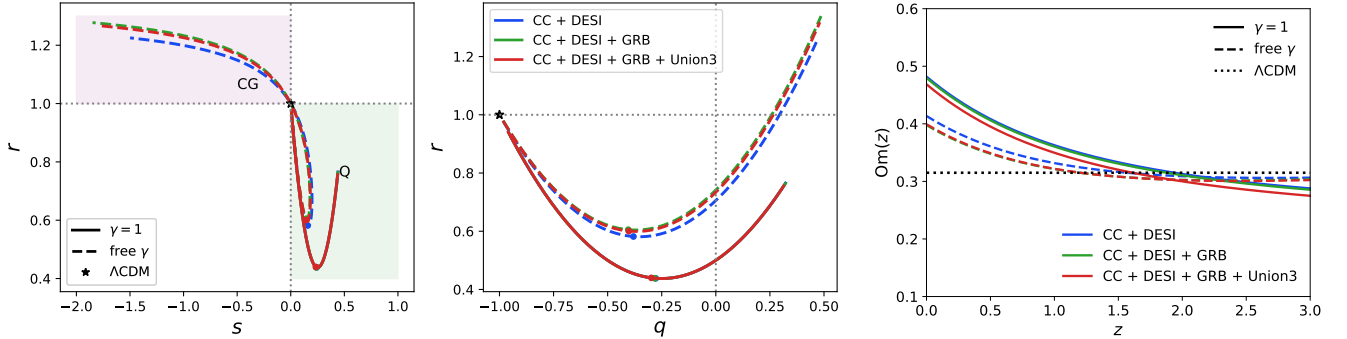


FIG. 9: Parametric trajectories in the (r, s) and (r, q) planes for the viscous model. The Chaplygin gas (CG) and quintessence (Q) regions are indicated for comparison. The $Om(z)$ diagnostic is also shown for the considered models, together with the Λ CDM prediction as a reference.

indicating that the present analysis does not fully alleviate the H_0 tension. Nevertheless, the moderate upward shift in H_0 preferred by the $f(Q)$ framework suggests that modified gravity effects may contribute nontrivially to the expansion history.

For the viscous model, the bulk viscosity coefficient is relatively large ($\zeta \sim 1.6$ for $\gamma = 1$ and $\zeta \sim 2.2$ for free γ), indicating that significant dissipative effects are required to sustain late-time acceleration within GR. In contrast, the exponential $f(Q)$ model achieves stronger acceleration with substantially smaller effective viscosity ($\zeta \sim 0.3$ –

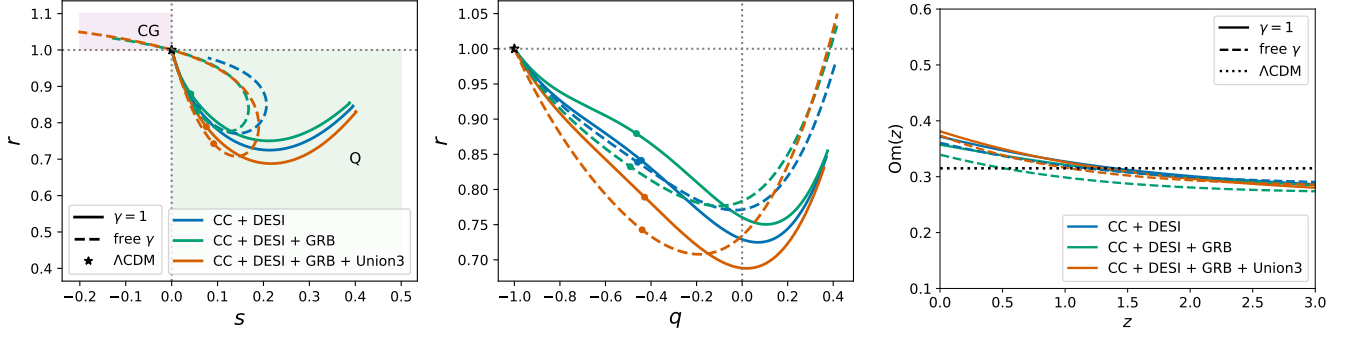


FIG. 10: Parametric trajectories of the exponential $f(Q)$ modified gravity model in the (r, s) and (r, q) statefinder planes. The Chaplygin gas (CG) and quintessence (Q) regions are indicated for comparison. The $Om(z)$ diagnostic is also shown for the considered models, together with the Λ CDM prediction as a reference.

Λ CDM Model

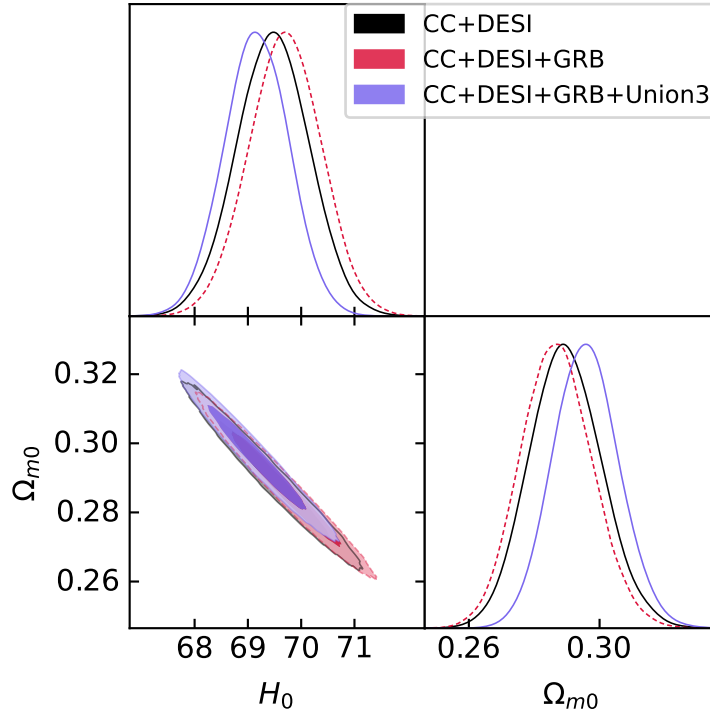


FIG. 11: The 1σ and 2σ likelihood contours for the Λ CDM model.

0.5) and values of γ close to unity. This demonstrates that the modified gravity contribution efficiently drives cosmic acceleration without requiring a strong departure from dust-like matter. The present-day deceleration parameter and effective equation of state confirm accelerated expansion in all cases, with the $f(Q)$ model systematically yielding more negative q_0 and $w_{\text{eff},0}$ than the purely viscous case. None of the models enter the phantom regime at the present epoch.

The geometrical diagnostics further clarify the dynamical behavior. In the (r, s) plane, the reconstructed trajectories approach the Λ CDM fixed point $(1, 0)$ at late times and evolve smoothly into the quintessence region toward higher redshift, remaining clearly separated from the Chaplygin gas sector. The (r, q) plane confirms a controlled transition from decelerated to accelerated expansion, with deviations from Λ CDM remaining moderate and well

TABLE II: Statistical comparison of viscous cosmology and viscous exponential $f(Q)$ gravity models relative to Λ CDM for different combinations of observational datasets. The quantities $\Delta\chi^2$, ΔAIC and ΔBIC are computed with respect to the corresponding Λ CDM case for the same dataset.

Model	χ^2_{\min}	AIC	BIC	$\Delta\chi^2$	ΔAIC	ΔBIC
CC + DESI						
Λ CDM	25.295	29.295	32.952	0	0	0
Viscous ($\gamma = 1$)	24.931	28.931	32.589	-0.364	-0.364	-0.363
Viscous (free γ)	22.250	28.250	33.735	-3.045	-1.045	+0.783
$f(Q)$ ($\gamma = 1$)	22.972	28.972	34.458	-2.323	-0.323	+1.506
$f(Q)$ (free γ)	22.275	30.275	37.589	-3.020	+0.980	+4.637
CC + DESI + GRB						
Λ CDM	265.605	269.605	276.280	0	0	0
Viscous ($\gamma = 1$)	266.906	270.906	277.581	+1.301	+1.301	+1.301
Viscous (free γ)	262.984	268.984	278.996	-2.621	-0.621	+2.716
$f(Q)$ ($\gamma = 1$)	264.040	270.040	280.052	-1.565	+0.435	+3.772
$f(Q)$ (free γ)	263.036	271.036	284.386	-2.569	+1.431	+8.106
CC + DESI + GRB + Union3						
Λ CDM	297.202	301.202	308.078	0	0	0
Viscous ($\gamma = 1$)	295.109	299.109	305.985	-2.093	-2.093	-2.093
Viscous (free γ)	288.258	294.258	304.572	-8.944	-6.944	-3.506
$f(Q)$ ($\gamma = 1$)	290.019	296.019	306.333	-7.183	-5.183	-1.745
$f(Q)$ (free γ)	288.280	296.280	310.033	-8.922	-4.922	+1.955

behaved. The $Om(z)$ diagnostic yields consistent conclusions.

A statistical comparison relative to Λ CDM is presented in Table II. For the CC + DESI dataset, all extended models remain statistically comparable to Λ CDM, as modest improvements in χ^2 are largely compensated by information-criterion penalties. However, when Union3 supernova data are included, the viscous model with free γ exhibits a significant reduction in χ^2 ($\Delta\chi^2 \approx -8.9$) and is favored by AIC, while remaining competitive under BIC. The exponential $f(Q)$ model also improves the fit, particularly for fixed γ , though the free- γ version is more strongly penalized by BIC due to the additional parameter freedom.

Overall, the extended viscous and exponential $f(Q)$ models remain statistically competitive with Λ CDM and, for the full dataset including Union3, yield notable improvements in goodness-of-fit. Nevertheless, viscous cosmologies continue to offer a physically motivated and viable alternative framework for explaining late-time acceleration. In particular, the statistical performance of the free- γ viscous model under the full dataset highlights its potential. To obtain more definitive conclusions, a natural next step is to extend the analysis by incorporating additional observations in the future, thereby providing stronger constraints on the early- and late-time dynamics and further testing the robustness of these models.

DATA AVAILABILITY

There are no new data associated with this article.

ACKNOWLEDGEMENTS

S.A. acknowledges the Japan Society for the Promotion of Science (JSPS) for providing a postdoctoral fellowship during 2024-2026 (JSPS ID No.: P24318). This work of S.A. is also supported by the JSPS KAKENHI grant (Number:

24KF0229). PKS acknowledges Science and Engineering Research Board, Department of Science and Technology, Government of India for financial support to carry out Research project No.: CRG/2022/001847 and IUCAA, Pune, India for providing support through the visiting Associateship program.

-
- [1] A. G. Riess, A. V. Filippenko, P. Challis, A. Clocchiatti, A. Diercks, P. M. Garnavich, R. L. Gilliland, C. J. Hogan, S. Jha, R. P. Kirshner, *et al.*, Observational evidence from supernovae for an accelerating universe and a cosmological constant, *The Astronomical Journal* **116**, 1009 (1998).
- [2] S. Perlmutter, M. S. Turner, and M. White, Constraining dark energy with type ia supernovae and large-scale structure, *Physical Review Letters* **83**, 670 (1999).
- [3] S. F. Daniel, R. R. Caldwell, A. Cooray, and A. Melchiorri, Large scale structure as a probe of gravitational slip, *Physical Review D* **77**, 103513 (2008).
- [4] T. Koivisto and D. F. Mota, Dark energy anisotropic stress and large scale structure formation, *Physical Review D* **73**, 083502 (2006).
- [5] H.-J. Seo and D. J. Eisenstein, Probing dark energy with baryonic acoustic oscillations from future large galaxy redshift surveys, *The Astrophysical Journal* **598**, 720 (2003).
- [6] C. Blake and K. Glazebrook, Probing dark energy using baryonic oscillations in the galaxy power spectrum as a cosmological ruler, *The Astrophysical Journal* **594**, 665 (2003).
- [7] A. G. Adame *et al.* (DESI), DESI 2024 VI: cosmological constraints from the measurements of baryon acoustic oscillations, *JCAP* **02**, 021, arXiv:2404.03002 [astro-ph.CO].
- [8] M. Abdul Karim *et al.*, DESI DR2 Results II: Measurements of Baryon Acoustic Oscillations and Cosmological Constraints (2025), arXiv:2503.14738 [astro-ph.CO].
- [9] N. Aghanim *et al.* (Planck), Planck 2018 results. VI. Cosmological parameters, *Astron. Astrophys.* **641**, A6 (2020), [Erratum: *Astron. Astrophys.* 652, C4 (2021)], arXiv:1807.06209 [astro-ph.CO].
- [10] I. Zlatev, L.-M. Wang, and P. J. Steinhardt, Quintessence, cosmic coincidence, and the cosmological constant, *Phys. Rev. Lett.* **82**, 896 (1999), arXiv:astro-ph/9807002.
- [11] S. Weinberg, The Cosmological Constant Problem, *Rev. Mod. Phys.* **61**, 1 (1989).
- [12] S. Capozziello, V. Cardone, and V. Salzano, Cosmography of $f(r)$ gravity, *Physical Review D* **78**, 063504 (2008).
- [13] T. P. Sotiriou and V. Faraoni, $f(r)$ theories of gravity, *Reviews of Modern Physics* **82**, 451 (2010).
- [14] A. De Felice and S. Tsujikawa, $f(r)$ theories, *Living Reviews in Relativity* **13**, 1 (2010).
- [15] T. Harko, F. S. Lobo, S. Nojiri, and S. D. Odintsov, $f(r, t)$ gravity, *Physical Review D* **84**, 024020 (2011).
- [16] H. Shabani and M. Farhoudi, Cosmological and solar system consequences of $f(r, t)$ gravity models, *Physical Review D* **90**, 044031 (2014).
- [17] Y.-F. Cai, S. Capozziello, M. De Laurentis, and E. N. Saridakis, $f(t)$ teleparallel gravity and cosmology, *Reports on Progress in Physics* **79**, 106901 (2016).
- [18] E. V. Linder, Einstein's other gravity and the acceleration of the universe, *Physical Review D* **81**, 127301 (2010).
- [19] S. S. Mishra, N. S. Kavya, P. K. Sahoo, and V. Venkatesha, Impact of Teleparallelism on Addressing Current Tensions and Exploring the GW Cosmology, *Astrophys. J.* **981**, 13 (2025).
- [20] D. Zhao, Covariant formulation of $f(q)$ theory, *The European Physical Journal C* **82**, 1 (2022).
- [21] N. Dimakis, A. Paliathanasis, M. Roumeliotis, and T. Christodoulakis, Flrw solutions in $f(q)$ theory: The effect of using different connections, *Physical Review D* **106**, 043509 (2022).
- [22] J. B. Jiménez, L. Heisenberg, T. Koivisto, and S. Pekar, Cosmology in $f(q)$ geometry, *Physical Review D* **101**, 103507 (2020).
- [23] F. D'Ambrosio, S. D. Fell, L. Heisenberg, and S. Kuhn, Black holes in $f(q)$ gravity, *Physical Review D* **105**, 024042 (2022).
- [24] S. Mandal, D. Wang, and P. Sahoo, Cosmography in $f(q)$ gravity, *Physical Review D* **102**, 124029 (2020).
- [25] I. S. Albuquerque and N. Frusciante, A designer approach to $f(q)$ gravity and cosmological implications, *Physics of the Dark Universe* **35**, 100980 (2022).
- [26] S. Capozziello and R. D'Agostino, Model-independent reconstruction of $f(q)$ non-metric gravity, *Physics Letters B* , 137229 (2022).
- [27] A. Lymperis, Late-time cosmology with phantom dark-energy in $f(q)$ gravity, *Journal of Cosmology and Astroparticle Physics* **2022** (11), 018.
- [28] N. Frusciante, Signatures of $f(q)$ gravity in cosmology, *Physical Review D* **103**, 044021 (2021).
- [29] G. N. Gadbail, S. Arora, P. Channuie, and P. K. Sahoo, Cosmological Dynamics of Interacting Dark Energy and Dark Matter in $f(Q)$ Gravity, *Fortsch. Phys.* **73**, 2400205 (2025), arXiv:2406.02026 [gr-qc].
- [30] A. Kolhatkar, S. S. Mishra, and P. K. Sahoo, Investigating early and late-time epochs in $f(Q)$ gravity, *Eur. Phys. J. C* **84**, 888 (2024), arXiv:2409.01538 [gr-qc].

- [31] L. Atayde and N. Frusciante, Can $f(q)$ gravity challenge λ cdm?, *Physical Review D* **104**, 064052 (2021).
- [32] R. Lazkoz, F. S. Lobo, M. Ortiz-Baños, and V. Salzano, Observational constraints of $f(q)$ gravity, *Physical Review D* **100**, 104027 (2019).
- [33] R. D'Agostino and R. C. Nunes, Forecasting constraints on deviations from general relativity in $f(Q)$ gravity with standard sirens, *Phys. Rev. D* **106**, 124053 (2022), [arXiv:2210.11935 \[gr-qc\]](#).
- [34] I. Ayuso, R. Lazkoz, and V. Salzano, Observational constraints on cosmological solutions of $f(q)$ theories, *Physical Review D* **103**, 063505 (2021).
- [35] B. J. Barros, T. Barreiro, T. Koivisto, and N. J. Nunes, Testing $f(q)$ gravity with redshift space distortions, *Physics of the Dark Universe* **30**, 100616 (2020).
- [36] F. K. Anagnostopoulos, S. Basilakos, and E. N. Saridakis, First evidence that non-metricity $f(q)$ gravity could challenge λ cdm, *Physics Letters B* **822**, 136634 (2021).
- [37] C. Eckart, The thermodynamics of irreversible processes. iii. relativistic theory of the simple fluid, *Physical review* **58**, 919 (1940).
- [38] J. Ren and X.-H. Meng, Modified equation of state, scalar field, and bulk viscosity in friedmann universe, *Physics Letters B* **636**, 5 (2006).
- [39] W. Israel and J. M. Stewart, Transient relativistic thermodynamics and kinetic theory, *Annals Phys.* **118**, 341 (1979).
- [40] P. P. Avelino, A. R. Gomes, and D. A. Tamayo, Note on bulk viscosity as an alternative to dark energy, *Phys. Rev. D* **112**, 123531 (2025), [arXiv:2512.15633 \[astro-ph.CO\]](#).
- [41] G. Palma and G. Gomez, Non-linear causal bulk viscosity in unified dark matter cosmologies, *Eur. Phys. J. C* **85**, 1486 (2025), [arXiv:2510.11900 \[gr-qc\]](#).
- [42] C. Singh and P. Kumar, Friedmann model with viscous cosmology in modified $f(r, t)$ gravity theory, *The European Physical Journal C* **74**, 1 (2014).
- [43] R. Solanki, S. Pacif, A. Parida, and P. Sahoo, Cosmic acceleration with bulk viscosity in modified $f(q)$ gravity, *Physics of the Dark Universe* **32**, 100820 (2021).
- [44] S. Arora, S. Pacif, A. Parida, and P. Sahoo, Bulk viscous matter and the cosmic acceleration of the universe in $f(q, t)$ gravity, *Journal of High Energy Astrophysics* **33**, 1 (2022).
- [45] I. Brevik, Crossing of the $w=-1$ barrier in viscous modified gravity, *International Journal of Modern Physics D* **15**, 767 (2006).
- [46] R. N. Villalobos, Y. Vásquez, N. Cruz, and C. H. López-Caraballo, Bulk viscous cosmological models with cosmological constant: Observational constraints, (2025), [arXiv:2508.11614 \[astro-ph.CO\]](#).
- [47] F. W. Hehl, P. Von Der Heyde, G. D. Kerlick, and J. M. Nester, General Relativity with Spin and Torsion: Foundations and Prospects, *Rev. Mod. Phys.* **48**, 393 (1976).
- [48] J. B. Jiménez, L. Heisenberg, and T. Koivisto, Coincident general relativity, *Physical Review D* **98**, 044048 (2018).
- [49] K. F. Dialektopoulos, T. S. Koivisto, and S. Capozziello, Noether symmetries in symmetric teleparallel cosmology, *The European Physical Journal C* **79**, 1 (2019).
- [50] J. B. Jiménez, L. Heisenberg, and T. S. Koivisto, Teleparallel palatini theories, *Journal of Cosmology and Astroparticle Physics* **2018** (08), 039.
- [51] T. K. Mathew, M. Aswathy, and M. Manoj, Cosmology and thermodynamics of flrw universe with bulk viscous stiff fluid, *The European Physical Journal C* **74**, 1 (2014).
- [52] Y. B. Zel'dovich, The equation of state at ultrahigh densities and its relativistic limitations, *Zh. Eksp. Teor. Fiz.* **41**, 1609 (1961).
- [53] K. R. Nair and T. K. Mathew, Bulk viscous Zel'dovich fluid model and its asymptotic behavior, *Eur. Phys. J. C* **76**, 519 (2016), [arXiv:1508.05041 \[gr-qc\]](#).
- [54] A. Avelino and U. Nucamendi, Can a matter-dominated model with constant bulk viscosity drive the accelerated expansion of the universe?, *JCAP* **04**, 006, [arXiv:0811.3253 \[gr-qc\]](#).
- [55] T. K. Mathew, M. B. Aswathy, and M. Manoj, Cosmology and thermodynamics of FLRW universe with bulk viscous stiff fluid, *Eur. Phys. J. C* **74**, 3188 (2014), [arXiv:1406.2089 \[gr-qc\]](#).
- [56] K. R. Nair and T. K. Mathew, Bulk viscous Zel'dovich fluid model and its asymptotic behavior, *Eur. Phys. J. C* **76**, 519 (2016), [arXiv:1508.05041 \[gr-qc\]](#).
- [57] F. K. Anagnostopoulos, S. Basilakos, and E. N. Saridakis, First evidence that non-metricity $f(Q)$ gravity could challenge Λ CDM, *Phys. Lett. B* **822**, 136634 (2021), [arXiv:2104.15123 \[gr-qc\]](#).
- [58] W. Khylllep, J. Dutta, E. N. Saridakis, and K. Yesmakhanova, Cosmology in $f(Q)$ gravity: A unified dynamical systems analysis of the background and perturbations, *Phys. Rev. D* **107**, 044022 (2023), [arXiv:2207.02610 \[gr-qc\]](#).
- [59] O. Sokoliuk, S. Arora, S. Praharaj, A. Baransky, and P. K. Sahoo, On the impact of $f(Q)$ gravity on the large scale structure, *Mon. Not. Roy. Astron. Soc.* **522**, 252 (2023), [arXiv:2303.17341 \[astro-ph.CO\]](#).
- [60] F. K. Anagnostopoulos, V. Gakis, E. N. Saridakis, and S. Basilakos, New models and big bang nucleosynthesis constraints in $f(Q)$ gravity, *Eur. Phys. J. C* **83**, 58 (2023), [arXiv:2205.11445 \[gr-qc\]](#).
- [61] S. Arora and P. K. Sahoo, Crossing Phantom Divide in $f(Q)f(Q)$ Gravity, *Annalen Phys.* **534**, 2200233 (2022), [arXiv:2206.05110 \[gr-qc\]](#).

- [62] D. Foreman-Mackey, D. W. Hogg, D. Lang, and J. Goodman, emcee: The mcmc hammer, *Publ. Astron. Soc. Pac.* **125**, 306 (2013).
- [63] A. Lewis, Getdist: a python package for analysing monte carlo samples, arXiv preprint arXiv:1910.13970 (2019).
- [64] H. Yu, B. Ratra, and F.-Y. Wang, Hubble parameter and baryon acoustic oscillation measurement constraints on the hubble constant, the deviation from the spatially flat Λ cdm model, the deceleration–acceleration transition redshift, and spatial curvature, *The Astrophysical Journal* **856**, 3 (2018).
- [65] M. Moresco, Raising the bar: new constraints on the Hubble parameter with cosmic chronometers at $z \sim 2$, *Mon. Not. Roy. Astron. Soc.* **450**, L16 (2015), arXiv:1503.01116 [astro-ph.CO].
- [66] R. Jimenez, L. Verde, T. Treu, and D. Stern, Constraints on the equation of state of dark energy and the Hubble constant from stellar ages and the CMB, *Astrophys. J.* **593**, 622 (2003), arXiv:astro-ph/0302560.
- [67] M. Moresco *et al.*, Improved constraints on the expansion rate of the Universe up to $z \sim 1.1$ from the spectroscopic evolution of cosmic chronometers, *JCAP* **08**, 006, arXiv:1201.3609 [astro-ph.CO].
- [68] M. Moresco, Raising the bar: new constraints on the Hubble parameter with cosmic chronometers at $z \sim 2$, *Mon. Not. Roy. Astron. Soc.* **450**, L16 (2015), arXiv:1503.01116 [astro-ph.CO].
- [69] M. Moresco, L. Pozzetti, A. Cimatti, R. Jimenez, C. Maraston, L. Verde, D. Thomas, A. Citro, R. Tojeiro, and D. Wilkinson, A 6% measurement of the Hubble parameter at $z \sim 0.45$: direct evidence of the epoch of cosmic re-acceleration, *JCAP* **05**, 014, arXiv:1601.01701 [astro-ph.CO].
- [70] N. S. Kavya, S. S. Mishra, and P. K. Sahoo, $f(Q)$ gravity as a possible resolution of the H_0 and S_8 tensions with DESI DR2, *Sci. Rep.* **15**, 36504 (2025).
- [71] M. Moresco, R. Jimenez, L. Verde, A. Cimatti, and L. Pozzetti, Setting the Stage for Cosmic Chronometers. II. Impact of Stellar Population Synthesis Models Systematics and Full Covariance Matrix, *Astrophys. J.* **898**, 82 (2020), arXiv:2003.07362 [astro-ph.GA].
- [72] J. Moon *et al.*, First detection of the BAO signal from early DESI data, *Mon. Not. Roy. Astron. Soc.* **525**, 5406 (2023), arXiv:2304.08427 [astro-ph.CO].
- [73] S. Alam *et al.* (eBOSS), Completed SDSS-IV extended Baryon Oscillation Spectroscopic Survey: Cosmological implications from two decades of spectroscopic surveys at the Apache Point Observatory, *Phys. Rev. D* **103**, 083533 (2021), arXiv:2007.08991 [astro-ph.CO].
- [74] D. Wang and D. Mota, Did DESI DR2 truly reveal dynamical dark energy?, (2025), arXiv:2504.15222 [astro-ph.CO].
- [75] G. Gu *et al.* (DESI), Dynamical dark energy in light of the DESI DR2 baryonic acoustic oscillations measurements, *Nature Astron.* **9**, 1879 (2025), [Erratum: *Nature Astron.* **9**, 1898 (2025)], arXiv:2504.06118 [astro-ph.CO].
- [76] S. S. Mishra, W. L. Matthewson, V. Sahni, A. Shafieloo, and Y. Shtanov, Braneworld dark energy in light of DESI DR2, *JCAP* **11**, 018, arXiv:2507.07193 [astro-ph.CO].
- [77] S. Arora, A. De Felice, and S. Mukohyama, Dynamical dark energy parametrizations in Λ CDM, *Phys. Rev. D* **112**, 123518 (2025), arXiv:2508.03784 [gr-qc].
- [78] S. S. Mishra, N. S. Kavya, P. K. Sahoo, and K. Bamba, DESI DR2 Meets Cosmography: A Comparative Study of Padé, Chebyshev, and Taylor Expansions, *Monthly Notices of the Royal Astronomical Society* **546**, stag197 (2026).
- [79] S. S. Mishra, N. S. Kavya, P. K. Sahoo, and T. Harko, Padé cosmography and its insights into teleparallel gravity, *Mon. Not. Roy. Astron. Soc.* **543**, 2816 (2025).
- [80] L. Amati *et al.*, Intrinsic spectra and energetics of BeppoSAX gamma-ray bursts with known redshifts, *Astron. Astrophys.* **390**, 81 (2002), arXiv:astro-ph/0205230.
- [81] M. Demianski, E. Piedipalumbo, D. Sawant, and L. Amati, Cosmology with gamma-ray bursts: II Cosmography challenges and cosmological scenarios for the accelerated Universe, *Astron. Astrophys.* **598**, A113 (2017), arXiv:1609.09631 [astro-ph.CO].
- [82] M. Demianski, E. Piedipalumbo, D. Sawant, and L. Amati, Cosmology with gamma-ray bursts: I. The Hubble diagram through the calibrated $E_{p,i} - E_{iso}$ correlation, *Astron. Astrophys.* **598**, A112 (2017), arXiv:1610.00854 [astro-ph.CO].
- [83] D. Rubin *et al.*, Union Through UNITY: Cosmology with 2,000 SNe Using a Unified Bayesian Framework, *Astrophys. J.* **986**, 231 (2025), arXiv:2311.12098 [astro-ph.CO].
- [84] J. Román-Garza, T. Verdugo, J. Magaña, and V. Motta, Constraints on barotropic dark energy models by a new phenomenological $q(z)$ parameterization, *The European Physical Journal C* **79**, 1 (2019).
- [85] J. Jesus, R. Valentim, A. Escobal, and S. Pereira, Gaussian process estimation of transition redshift, *Journal of Cosmology and Astroparticle Physics* **2020** (04), 053.
- [86] A. Al Mamon and K. Bamba, Observational constraints on the jerk parameter with the data of the hubble parameter, *The European Physical Journal C* **78**, 1 (2018).
- [87] V. Sahni, T. D. Saini, A. A. Starobinsky, and U. Alam, Statefinder—a new geometrical diagnostic of dark energy, *Journal of Experimental and Theoretical Physics Letters* **77**, 201 (2003).
- [88] U. Alam, V. Sahni, T. Deep Saini, and A. Starobinsky, Exploring the expanding universe and dark energy using the statefinder diagnostic, *Monthly Notices of the Royal Astronomical Society* **344**, 1057 (2003).

- [89] V. Sahni, A. Shafieloo, and A. A. Starobinsky, Two new diagnostics of dark energy, *Phys. Rev. D* **78**, 103502 (2008).
- [90] S. Pan, A. Mukherjee, and N. Banerjee, Astronomical bounds on a cosmological model allowing a general interaction in the dark sector, *Monthly Notices of the Royal Astronomical Society* **477**, 1189 (2018), <https://academic.oup.com/mnras/article-pdf/477/1/1189/24703456/sty755.pdf>.